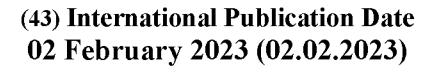
(12) INTERNATIONAL APPLICATION PUBLISHED UNDER THE PATENT COOPERATION TREATY (PCT)

(19) World Intellectual Property Organization

International Bureau







(10) International Publication Number WO 2023/009355 A1

- (51) International Patent Classification: *G01S 11/08* (2006.01) *G01S 5/02* (2010.01)
- (21) International Application Number:

PCT/US2022/037622

(22) International Filing Date:

19 July 2022 (19.07.2022)

(25) Filing Language:

English

(26) Publication Language:

English

(30) Priority Data:

63/226,625

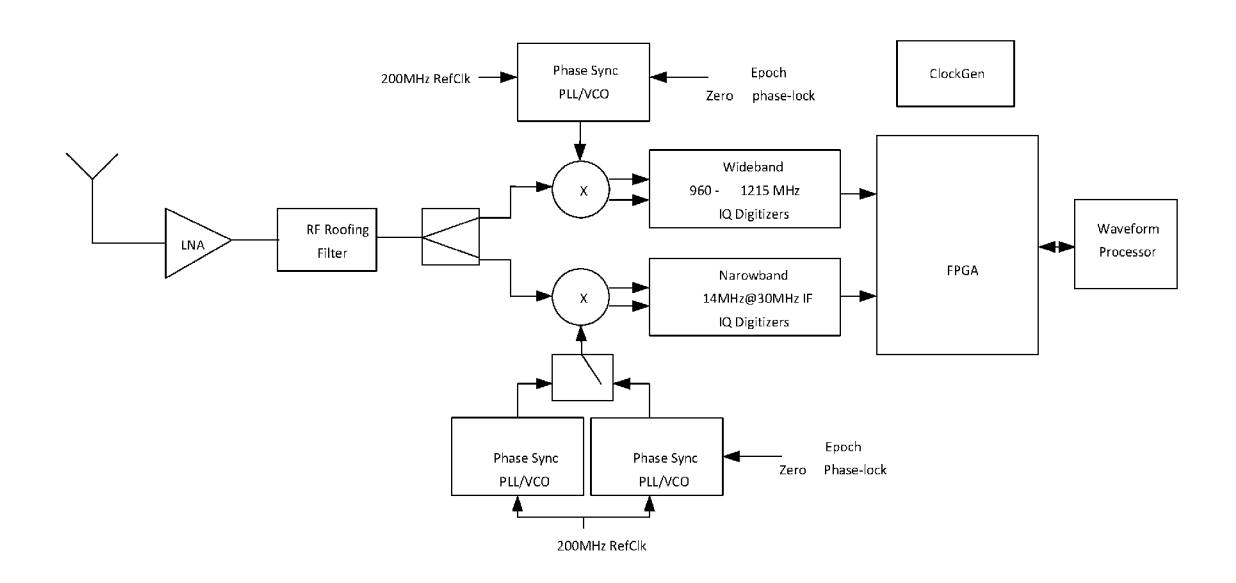
28 July 2021 (28.07.2021)

TIC

- (71) Applicant: VIASAT, INC. [US/US]; c/o Patent Department, 6155 El Camino Real, Carlsbad, California 92009 (US).
- (72) Inventor: HOU, Yoshen; Viasat, Inc., c/o Patent Department, 6155 El Camino Real, Carlsbad, California 92009 (US).
- (74) Agent: BURRASTON, N., Kenneth et al.; Viasat, Inc., c/ o Patent Department, 6155 El Camino Real, Carlsbad, California 92009 (US).

- (81) Designated States (unless otherwise indicated, for every kind of national protection available): AE, AG, AL, AM, AO, AT, AU, AZ, BA, BB, BG, BH, BN, BR, BW, BY, BZ, CA, CH, CL, CN, CO, CR, CU, CV, CZ, DE, DJ, DK, DM, DO, DZ, EC, EE, EG, ES, FI, GB, GD, GE, GH, GM, GT, HN, HR, HU, ID, IL, IN, IQ, IR, IS, IT, JM, JO, JP, KE, KG, KH, KN, KP, KR, KW, KZ, LA, LC, LK, LR, LS, LU, LY, MA, MD, ME, MG, MK, MN, MW, MX, MY, MZ, NA, NG, NI, NO, NZ, OM, PA, PE, PG, PH, PL, PT, QA, RO, RS, RU, RW, SA, SC, SD, SE, SG, SK, SL, ST, SV, SY, TH, TJ, TM, TN, TR, TT, TZ, UA, UG, US, UZ, VC, VN, WS, ZA, ZM, ZW.
- (84) Designated States (unless otherwise indicated, for every kind of regional protection available): ARIPO (BW, GH, GM, KE, LR, LS, MW, MZ, NA, RW, SD, SL, ST, SZ, TZ, UG, ZM, ZW), Eurasian (AM, AZ, BY, KG, KZ, RU, TJ, TM), European (AL, AT, BE, BG, CH, CY, CZ, DE, DK, EE, ES, FI, FR, GB, GR, HR, HU, IE, IS, IT, LT, LU, LV, MC, MK, MT, NL, NO, PL, PT, RO, RS, SE, SI, SK, SM, TR), OAPI (BF, BJ, CF, CG, CI, CM, GA, GN, GQ, GW, KM, ML, MR, NE, SN, TD, TG).

(54) Title: PRECISION TIME AND DISTANCE MEASUREMENT UTILIZING A TACTICAL DATA LINK RADIO



Fia. 5

(57) **Abstract:** Techniques for determining time-of-arrival (TOA), at a radio receiver, of a radio signal transmitted in the form of a series of coded pulses on each of a plurality of radio channels having distinct channel frequencies, where the coded pulses are transmitted coherently.

Published:

— with international search report (Art. 21(3))

PRECISION TIME AND DISTANCE MEASUREMENT UTILIZING A TACTICAL DATA LINK RADIO

TECHNICAL FIELD

This disclosure is generally related to radio receivers and is more particularly related to estimating a time-of-arrival (TOA) of a radio signal at a radio receiver, for the purpose of determining a distance between the radio receiver and a transmitter of the radio signal.

BACKGROUND

Link 16 is a tactical data link (TDL) network used by militaries around the world. Link 16 is a TDMA-based digital data link operating in the 960 – 1215 MHz radio frequency band, and utilizes frequency hopping to provide secure, jam-resistant, and high-speed data communications between line-of-sight users.

In many scenarios where TDL or other multi-channel frequency-hopping radio links are used, it would be useful to precisely estimate the propagation time of signals from the transmitter to the receiver, e.g., for the purpose of estimating the distance between the radio link users. Due to the complexity of the multi-channel frequency-hopping signals, this is difficult to do. A measurement based on a single one of the multiple channels can be used to generate a timing estimate, but a high-precision estimate is often not possible because the bandwidth of the single channel is too narrow and the duration of the signal on that channel is too short. Averaging timing estimates obtained from multiple channels is possible but still may not yield enough precision.

SUMMARY

Various embodiments of the techniques and apparatuses described herein provide for precise measurement of the time-of-arrival of a radio signal at a receiver, for radio signals transmitted in the form of a series of coded pulses on each of a plurality of radio channels having distinct channel frequencies. This time-of-arrival can then be used to estimate a distance between the transmitter of the radio signal and the receiver.

Embodiments described herein include methods for determining time-of-arrival (TOA), at a radio receiver, of a radio signal transmitted in the form of a series of coded pulses on each of a plurality of radio channels having distinct channel frequencies, where the coded pulses are transmitted coherently, i.e., with a known relationship between the phases of the signals on

each channel. Example techniques comprise calculating an initial estimate of the TOA using non-coherent combining of timing information obtained from detected preamble sequences and calculated refined estimates of the TOA estimate or of error in the TOA estimate using code phase information obtained from multiple ones of the radio channels.

Also described herein are example radio receivers configured to carry out one or more of the various techniques disclosed herein.

Of course, the present invention is not limited to the above features. Indeed, those skilled in the art will recognize additional features and advantages upon reading the following detailed description, and upon viewing the accompanying drawings.

BRIEF DESCRIPTION OF THE DRAWINGS

Figure 1 illustrates an example TDL handheld phase-coherent fast-hop transmitter.

Figure 2 illustrates an example of phase-coherent transmitter clock timing.

Figure 3 shows an example of TX LO phase alignment, with MSK modulation, which can be used to support precision distance measurement according to the techniques described herein.

Figure 4 illustrates an example of TDL MSK/GMSK (Gaussian minimum shift keying) encoded data phases and zero-phase Link-16 pulse epoch time.

Figure 5 is a block diagram of an example TDL (e.g., Link-16) handheld receiver capable of precision distance measurement.

Figure 6 is a top-level functional block diagram of an example preamble searcher.

Figure 7 is a block diagram of an example implementation of a CCSK correlator.

Figure 8 shows an example auto-correlation of an MSK-modulated CCSK-encoded pulse with a PN cover.

Figure 9 illustrates results of an example preamble search, with a TOA estimation error, and the correlation output of the CCSK encoded pulse.

Figure 10 shows sampled symbol phases for RF pulses that have a small timing error in symbol alignment.

Figure 11 illustrates an example of decoded CCSK code phases, with TOA error.

Figure 12 shows an example of wide-lane zero-phase TOA position fix, according to some embodiments of the presently disclosed techniques.

Figure 13 is a process flow diagram illustrating an example method for determining a TOA estimate, according to several embodiments of the presently disclosed techniques.

Figure 14 is a block diagram illustrating an example radio receiver configured to carry out one or more of the techniques described herein.

DETAILED DESCRIPTION

This disclosure describes examples of an architecture for tactical data link (TDL) (e.g., Link-16) radios that can be used to achieve precision distance measurements. The enhancements described herein can be backward compatible with legacy TDL operation in hardware and/or software. Furthermore, the techniques described herein can be applied more generally, to systems using radio links characterized by the use of coded pulses sent over multiple radio channels, in a frequency-hopping manner.

Precision timing measurements, which can be readily converted into distance measurements, can be achieved by coherently combining phase/timing information obtained from multiple pulses, received on multiple radio channels. By "coherently combining" is meant that the combining of the information from the signals received on the multiple channels is combined in such a way that takes into account or exploits the fact that the phase relationship between the phases of the radio signals on the different channels is known. This has the effect of converting several narrow-band measurements, which each individually only allow for a coarse estimate of signal timing, into a wide-band, high-precision measurement, exploiting most or all of the channels used by the system.

One key to the techniques described herein is the availability of a transmitter architecture that supports transmission of the coded pulses in such a manner that radio carrier phase coherence, with respect to transmitter reference, is maintained from one pulse to another, even as the carrier frequency for the channel occupied by the pulse changes. The following discussion provides a description of such an architecture.

Another key is the ability to resolve ambiguities resulting from "phase wrap-around." When noisy phase measurements are performed on two pulses transmitted at different times, for example, a phase difference between these pulses can be calculated. This phase difference is related to the difference in timing between the pulses. However, when precise timing and precise Doppler shift information is unknown, such a calculation has an inherent ambiguity with respect to the number of 360-degree cycles that occurred between the two measurements. The techniques described herein resolve these phase wrap-around ambiguities using a novel, iterative technique for combining phase/timing information obtained from coded pulses transmitted over multiple radio channels.

Figure 1 is a functional block diagram illustrating an example TDL (e.g., Link-16) transmitter designed to provide phase coherency between pulses transmitted on different ones of multiple frequency-hopping radio channels. Elements of this example configuration include fast-locking PLLs (phase-locked loops) that are capable of LO (local oscillator) phase steering while remaining frequency locked to a system reference clock (e.g., 200 MHz) in a fractional mode. After frequency lock, the PLL/VCO (voltage-controlled oscillator) can achieve phase lock with an RF (radio frequency) LO output phase aligned to an epoch time (e.g., a 2 us (microsecond) epoch time) of each pulse period (e.g., 13 us). The overall phase lock time for each PLL/VCO, i.e., the time to achieve frequency lock and then phase lock, can be low, e.g., 12 us. Because of the added lock time needed for phase steering, the TXLO (transmit local oscillator) can be produced using a ping-pong switching structure of two PLL/VCOs. This can result in each pulse period having a stable TX (transmit) LO during RF pulse data modulation.

A TDL handheld transmitter like the one shown in Figure 1 can utilize direct conversion transmission where the transmit DACs (digital-to-analog converter) produce baseband IQ analog signals. A single up-conversion mixer can bring the signal to be transmitted directly up to any one of the 51 TX LO carrier frequencies defined for the Link 16 system. An advantage of combining the direct-conversion transmitter and phase-locked TX LO is that the transmitter output can maintain phase coherency while in TDL fast hopping operation. Both the transmit modulation and the TXLO PLL reference clocks can be sourced from a single reference clock oscillator.

Figure 2 shows an example of detailed transmitter clock timing that can support precision distance measurement. The illustrated example is based on the legacy Link-16 waveform,

but it will be appreciated that the concepts discussed herein are not limited to the particular frequencies, timings, and signal formats utilized in Link 16.

The Link 16 radio signal comprises data sent in the form of a series of coded pulses, where each pulse is transmitted on one of 51 3-MHz-wide channels and where the transmitter hops from one channel to the next between pulses. The pulse interval is 13 microseconds, where this interval consists of a 6.4-microsecond on-time and a 6.6-microsecond off-time. During its on-time, the pulse is Minimum-Shift-Keying (MSK) modulated with chips at a 5-MHz chip rate – thus, the pulse on-time encompasses 32 chips. Cyclic code-shift keying (CCSK) can be used, to encode a 5-bit symbol value into the 32-chip sequence carried by a pulse.

The transmitter timing circuit can be controlled to be coherent to the RF LO phase. In other words, the transmitter timing can be controlled so that the leading and trailing edges of the transmitted pulse, as well as the beginning and end of each chip, have a consistent and stable relationship to the phase of the RF LO, across pulses.

All the clocks in the transmitter can be sourced and phase locked to the OCXO/TCXO (e.g., oven or temperature-controlled crystal oscillator) circuit system clock. A system clock (e.g., 5 MHz) can drive the TDL chip symbols. The main pulse-alignment time instant can be defined as a particular amplitude position on a first chip, e.g., the "zero-phase" time can be established at the instant the first chip pulse amplitude reaches 95% of its peak amplitude. This "zero-phase" time can be assigned to be a set time period (e.g., 2 us) from the start of the repetitive pulse period.

Figure 3 depicts an example of how the TX LO phase can be aligned with TX data modulation in a constellation map. As seen in the figure, a zero-phase reference position for the TX LO is defined, e.g., with reference to the first chip of the coded Link 16 pulse. In this example, a rising ramp-up tone at -1.25 MHz relative to the channel center frequency precedes the zero-phase reference position. The phase of the transmitted signal, relative to the TX LO, thus rotates in a clockwise manner. A series of 32 MSK-encoded chips follows the zero-phase reference position – these chips each shift the phase of the signal clockwise or counter-clockwise, according to the illustrated MSK constellation. The 32 chips are followed by a trailing ramp-down tone, at +1.25 MHz relative to the carrier frequency, which rotates the phase of the signal in a counter-clockwise manner.

Figure 4 shows an example of the time-domain waveform for the IQ modulation used to generate the transmitted signal. In this example, the rising edge of each RF burst, or pulse, is a continuous-wave (CW) tone at one frequency offset from the carrier frequency (e.g., - 1.25MHz), while the falling edge is a CW tone at a second offset from the carrier frequency (e.g., +1.25MHz). The zero-LO phase reference point can be defined at the beginning of the first chip of the MSK modulation (e.g., at 95% of amplitude point). Equivalently, that also can define code phases of multi-chip (e.g., 32-chip) TX pulse symbols. In other words, each chip can be characterized as having a particular code phase, relative to the TX LO.

Once transmit clock timing and RF LO phases are aligned, a zero-distance reference point can be defined, e.g., at the center of an antenna port. As noted above, the zero-distance time reference can be, for example, at 95% amplitude of the first preamble pulse with zero RF code phase. Currently, the legacy Link-16 TDLs define a zero-distance reference point to be the first-chip position with 95% amplitude of the first preamble pulse. In these legacy systems, there need not be an alignment of the RF LO phase.

Figure 5 shows a top-level block diagram of an example TDL radio receiver that can be used to carry out the techniques described herein. The example shown features a 960-1215 MHz wideband staring receiver (WBRX) capable of receiving all Link-16 operating frequency channels at the same time, as well as a narrowband 14-MHz bandpass receiver (NBRX) having an intermediate frequency (IF) of 30MHz. In the example, both receivers are driven by phase-synchronized PLL/VCOs. The WBRX can allow tuning and detection of the 32 pulses of a preamble sequence, transmitted on a predetermined eight of the 3-MHz-wide radio channels. Immediately after preamble detection, data pulses can either be demodulated by the WBRX or the receiver may transition to the NBRX for better anti-jam protection. Like the transmitter, the NBRX can be driven by a ping-ponged, phase-synchronized, RX LO and thus, in the same manner as described above for the transmitter, to achieve zero-phase at Link-16 reference clock.

To begin, the TDL (e.g., Link-16) demodulator core, which can be implemented in the FPGA of the receiver shown in Figure 5, for example, can be loaded with a known preamble sequence of multiple pulses (e.g., 32), with each pulse in the sequence having multiple chips (e.g., 32) per pulse, where the pulses are transmitted over multiple (e.g., 8) TDL carrier frequencies. WBRX can perform multiple-channel tuning (e.g., 8-channel tuning) to the predetermined preamble carrier frequencies.

Figure 6 shows an example of a preamble searcher functional block diagram. Because the clock timing difference between the transmitter and receiver and the Doppler shift undergone by the transmitted signal is unknown initially, these pulses (e.g., 32) can be non-coherently combined. In other words, the code phase for each of the preamble pulses can be ignored, with the pulses being delay shifted and combined for hypothesis testing, to detect the preamble sequence and its coarse timing.

Detection of the preamble sequence can provide time-of-arrival (TOA) information of the received pulses, and thus provide timing information for the transmitted signal. Performing preamble detection at the Nyquist rate (e.g., 5 MHz in this example) can facilitate the TDL demodulator achieving coarse estimation with limited hardware logic resources, which may be particularly important with a programmable gate array (FPGA) implementation. Transmit symbol timing alignment can be performed by refining and interpolating from the samples, which in this example can be 5-Mhz samples.

Due to filtering and bandwidth limiting, the cross-correlation curve of the preamble detection may span several symbols and the peak position may be smeared. Upon cross-correlating with a known sequence at the Nyquist sampling rate, the true peak position can be interpolated, which can achieve sub-chip accuracy, i.e., an accuracy of better than 200 nanoseconds, given a 5-MHz chip rate. But, interpolation may have limited reconstructing capability, dependent on signal conditions, so there may be uncertainty.

Non-coherent preamble combining as described above lacks accuracy because all RF code phases are ignored. The information provided by the RF code phases is eliminated from the calculation, by squaring. Nevertheless, the coarse TOA acquisition achieved with the non-coherent combining can serve well for aligning at the scale of the TX chip symbols (e.g., of 200ns). 200-nanosecond accuracy, however, corresponds to errors of up to 200 feet, for distance estimation. For precision distance measurements, demodulated TX pulse code phases can be used to refine the TOA accuracy down to a fraction of the carrier RF wavelength. For carrier frequencies of about 1 GHz, as in the TDL system, the carrier period is about 1 nanosecond, corresponding to a wavelength of about 1 foot.

What is needed, however, is an efficient method to resolve the phase ambiguities that inherently arise when evaluating phase differences between multiple received pulses.

Following are details of a technique for iteratively incorporating phase information obtained from pulses to refine the TOA estimate.

TDLs typically transmit RF pulses that pseudo-randomly hop among multiple carrier frequencies. For example, the signal transmitted by a Link-16 TDL can be composed of RF pulses (72 for Link 16's round-trip time (RTT) transmission, 258 for standard data (STD) or Packed-2 Single Pulse (P2SP) transmissions, and 444 for Packed-2 Double Pulse (P2DP) or P4/ET0-4 transmissions) that pseudo-randomly hop among 51 carrier frequencies. Each RF pulse can comprise 32 pseudo-random 5MHz chips that are MSK modulated, for a 6.4us burst length.

Given this baseline, let r(t) represent the base-band equivalent signal, as down-converted from the WBRX RX LO and IQ demodulated. The receive signal at the antenna port can be expressed as:

$$r(t) = Ae^{j\varphi} \sum_{n=0}^{n-1} S_n(t - nT_P - T_D)e^{j\omega_n(t - T_D)} + v(t), \tag{1}$$

where $S_n(t)$ is the MSK-modulated TX symbol for pulse n, T_P is the 13 us pulse period, T_D is the propagation delay, $Ae^{j\varphi}$ is the path attenuation (φ =0 for line-of-sight), ω_n is the carrier frequency for pulse n, ω_R is the WBRX RX LO frequency, and v(t) is the receiver noise.

In the situation where the transmit source terminal experiences clock drift and/or Doppler shift, the transmitted carrier frequency may be slightly altered from its nominal value. For Doppler shift, the effect can be described as:

$$\omega_n' = \left(1 + \frac{\Delta v}{c}\right)\omega_n = (1 + f_V)\omega_n \qquad . \tag{2}$$

For frequency deviation f_D (in ppm) that results from clock inaccuracy, the effect of clock compression on the source terminal can be:

$$t' = (1 + f_D)t \tag{3}$$

Assuming the receiver has perfect timing source, the receive signal at the antenna port can be expressed as:

$$r(t) = Ae^{j\varphi} \sum_{n=0}^{n-1} S_n(t' - nT_P' - T_D)e^{j\omega_n'(t' - T_D)} + v(t)$$
 (4)

Assume a preamble sequence has been detected and TOA/TX symbol timing has an estimation error of ΔT from the coarsely estimated T_D TOA. After digitally sampling and

baseband filtering, the combined result on receive signal digitization after digital down-conversion of the RX LO at angular frequency ω_R can be given as:

$$r(k) = Ae^{j\varphi} \sum_{n=0}^{n-1} S_n (kT_s + \Delta T - nT_P - T_D) e^{j\{\omega'_n[(1+f_D)(kT_s + \Delta T) - T_D] - \omega_R(kT_s + \Delta T)\}} + v(kT_s),$$
(5)

where T_S is the sampling time.

Continuing with the foregoing Link-16 example, the demodulator core can perform PN (pseudo noise) de-covering, if needed, and CCSK (cyclical code shift keying) symbol detection. Assuming correct CCSK demodulation, the CCSK correlator output can be expressed as:

$$C(n) = \frac{Ae^{j\varphi}}{L} \sum_{k=0}^{L-1} r(k) S_n^* (kT_S - nT_P - T_D) e^{-j\{\omega_n(kT_S - T_D) - \omega_R kT_S\}} + N_n.$$
 (6)

The parameters f_V and f_D can have small values, so the $f_V f_D$ term is negligible and can be removed from computation, for simplification. Equation (6) can be simplified to:

$$C(n) = Ae^{j\varphi}R_n(\Delta T)e^{j[n(f_V + f_D)\omega_n T_P + [(1 + f_V + f_D)\omega_n - \omega_R)\Delta T - f_V\omega_n T_D]} + N_n, \qquad (7)$$

where $R_n(\Delta T)$ is the autocorrelation of the MSK modulated TX symbols, given by:

$$R_n(\Delta T) = \frac{1}{L} \sum_{k=0}^{L-1} S_n(kT_s + \Delta T) S_n^*(kT_s) \qquad , \tag{8}$$

and L is the number of samples per pulse period. The pulse period T_P is LT_s .

Figure 7 shows an example of an implementation of CCSK demodulation, which can be implemented in firmware, e.g., in the waveform signal processor shown in Figure 5, or in digital hardware, e.g., using the FPGA shown in that same figure. In the illustrated example, the PN cover is removed from the 32-chip TX symbols. Then, the received chip symbols are correlated against each of the 32 CCSK sequences. The correlation result having the peak amplitude (maximum likelihood) is flagged as indicating the decoded CCSK code.

Once CCSK decoding is completed, the code phase for pulse n can be detected as:

$$\Psi(n) = \varphi + n(f_V + f_D)\omega_n T_P + [(1 + f_V + f_D)\omega_n - \omega_R)\Delta T - f_V \omega_n T_D + N_{\phi}(n). \tag{9}$$

Notice the TOA estimation term ΔT may degrade the detected CCSK code phase from the phase term of $R_n(\Delta T)$. Figure 8, which illustrates a simulation of amplitude and phase distortion of MSK modulated CCSK with PN cover, illustrates the impact of this degradation. Amplitude may change significantly over TOA estimation errors of up 200-300 nanoseconds. But, phase typically changes negligibly for initial TOA errors of within a duration of about one-half chip (e.g., -100 ns,100 n).

Based on the derivation of Equation (9) and given the availability of CCSK code-phase measurements of Link-16 pulse symbols, a method of refining TOA estimation to achieve a precision timing and/or distance measurement can be determined. This method is detailed below. First, a technique for estimating Doppler shift and clock drift is described. Then, a technique for precision TOA-timing estimation is provided.

A clock phase measured in a typical TDL (e.g., Link-16) demodulator can be expressed as in Equation (9). A problem related to angle measurement may be the uncertainty of 2π wrapping, i.e., the ambiguities caused by the unknown number of 360-degree phase rotations that have occurred between two moments in time. To mitigate the problem of uncertainly, we can devise the receiver structure. In the case of a Link-16 example:

A. Set WBRX RX LO to Channel 19 carrier frequency of 1,113 MHz. Equivalently ω_R =1113 MHz and $\omega_{I9} - \omega_R$ =0.

Channel 19 is the closest Link-16 operating channel to the middle of the 969-1206 MHz operating band of the system. By choosing WBRX RXLO to be 1,113 MHz, the initial code phase measurement, using Equation (9), is devoid of TOA estimation error. For small Doppler shift, at channel 19, code phase detection reduces to

- B. Collect RF pulses on Channel 19. Code phases are $\Psi(n) = \varphi + n(f_V + f_D)\omega_n T_P f_V\omega_n T_D + N_{\phi}(n)$ for all pulses on Channel 19 (HopCh of n=19). Compute the slope of the code phases across time, which vary with the sparse pulse position n. The resulting slope is the mean value of $(f_V + f_D)\omega_n T_P$. As to wrap-around phase uncertainty, a typical 0.1-ppm clock produces 0.1ppm*1113MHz*200*13e-6=29% cycles of uncertainty over a period containing 200 RF pulse periods. It is thus technically feasible to resolve phase wrapping uncertainty.
- C. To refine measurement of frequency deviation, repeat step B iteratively, using the previously estimated $(f_V + f_D)$, on Link-16 channels from Ch20 to Ch50 using Equation (9). Perform averaging of $(f_V + f_D)$ estimate to reduce noise contribution.

The frequency deviation and Doppler shift measured using the above procedure can then be removed from the code phase measurements. For simplicity, Equation (9) can then be rewritten as:

$$\Psi(n) = \varphi + [(1 + f_V + f_D)\omega_n - \omega_R]\Delta T - f_V \omega_n T_D + N_{\phi}(n)$$
(10)

Continuing with the Link-16 example above, the method to measure ΔT , i.e., the error in the initial TOA estimate, utilizes wide-lane ambiguity resolution starting from low frequency to high frequency phase rotation. The technique proceeds as follows:

- D. After correction of $(f_V + f_D)$ term, re-compute all code phases, and then, for each carrier channel for which code phases have been measured and re-computed, average code phases obtained from the same carrier channel.
- E. Start with channel 19, where $\omega_{19}=\omega_R=1,113$ MHz. The average code phase for this channel forms the estimate of path attenuation phase $\varphi f_V \omega_n T_D$, where $\hat{\varphi} = avg\{\Psi(n|n\ eq\ 19)\}$.
- F. Perform a second iteration with Channel 20, where ω_{20} - $\omega_R = 3$ MHz. The low frequency-wideband allows a first estimate of TOA error as $\Delta \widehat{T(0)} = \frac{avg\{\Psi(n|n\ eq\ 20)\}-\widehat{\varphi}}{[(1+f_V+f_D)\omega_{20}-\omega_R]}$.
- G. Iterate across Channels 21-50 and Channels 0-18, in such a way that there is a gradual increase of ω_n - ω_R . For each iteration, compute and update TOA error estimate as $\Delta T(k+1) = \Delta T(k) + \beta \frac{avg\{\Psi(n|n\ eq\ W(k))\}-((1+f_V+f_D)\omega_{W(k)}-\omega_R)\Delta T(k)-\widehat{\phi}}{[(1+f_V+f_D)\omega_{W(k)}-\omega_R]}.$ W(k) is the wide lane Link-16 channel list that sequences from lowest to highest frequency offset for phase ambiguity resolution. For the Link 16 system, this list may go as follows: W=[(19:35),18,36,17,37,16,38,15,39,14,(40:50),13:0)]. β is an adaptation coefficient, and is selected to be between 0 and 1. It acts to control the digital integration of the updates of measurement errors. For lower beta, new updates of error will not change the refined error estimate as quickly, at the expense of slower convergence. Higher beta will be integrated into the estimated error more quickly, but will create noisier results. The appropriate level may be determined from experiment.

The following test shows typical results of precision TOA estimation. Figure 9 shows an example of a successful preamble sequence acquisition, but where the initial TOA estimate has 34 ns of error. This slight timing error has a negligible impact on CCSK decoding and all

TX symbols can thus be successfully decoded. CCSK IQ code phases are processed and saved for precision TOA estimation.

Figure 10 shows the CCSK sampled phases of all RF pulses that have a slight timing error of symbol alignment. The TOA error induces code phase errors, with the magnitude of those errors depending on the frequency offset from RX LO of the channels on which the code phases are measured. Figure 11 shows an example of resulting CCSK code phase errors for all 51 channels of the Link 16 system. Behaviors of these code phase errors follows the mathematical description given in Equation (10). The "wide lane" ambiguity resolution technique described above can be used to mitigate effect of 2π phase wrapping uncertainty. An example of results of wide lane processing and adaptation is shown in Figure 12. An example of results of CCSK code phase correction from TOA fine adjustment is shown on the right of Figure 12.

Figure 13 is a process flow diagram illustrating an example method, according to several of the techniques described herein, for determining, in a radio receiver, time-of-arrival (TOA) of a radio signal transmitted in the form of a series of coded pulses on each of a plurality of radio channels having distinct channel frequencies. It should be understood that this method is a generalization of the specific examples described above, in that the techniques described herein are not limited to the particular frequencies and channel structures of Link 16, but are more generally applicable to systems in which coded pulses are sent on multiple radio channels, while maintaining phase coherency between the pulses.

As shown at block 1310, the method comprises the step of estimating a coarse TOA for the received radio signal, by detecting preamble sequences in each channel of a first set of the channels, non-coherently combining the detected preamble sequences, and estimating timing for a peak resulting from the non-coherent combining. In the context of the Link 16 system, this first set of channels may be all or some of the channels in which preamble pulses/sequences are sent. In other systems, this first set may include any channels in which known sequences or one or more of a limited number of possible sequences are transmitted.

Details of this process were described above. Note that the coarse TOA estimated here is, effectively, an estimate of T_d , the propagation delay from the transmitter to the receiver. At this point, there may be unknown frequency differences between the reference clocks in the transmitter and receiver, and the Doppler shift imposed on the transmitted signal is unknown.

As was discussed above, this coarse estimation of the TOA bounds the estimation error to a sub-chip level, e.g., less than 200 nanoseconds. Subsequent steps in the illustrated method are focused on estimating the error, ΔT , in this initial estimate, by exploiting the additional information available from the phase coherency between coded pulses, thereby refining the TOA estimate.

As shown at block 1320, the method further comprises performing symbol detection for each of a plurality of the coded pulses, on each channel of a second set of the channels, and estimating a code phase for each of the coded pulses, based on the symbol detection. This second set of the channels may be distinct from the first set, or partially or fully overlap the first set, in various implementations. As discussed above, the code phases of the coded pulses in the radio signal as transmitted are coherently related across time and across the plurality of radio channels – this characteristic of the transmitted signal enables the coherent combination of code phase information from multiple pulses, as carried out in the subsequent steps of the method.

In some, but not necessarily all, implementations, the coded pulses are cyclic code-shift keying (CCSK) -coded pulses. In these implementations, performing symbol detection for each of the plurality of coded pulses may comprise, for each of the coded pulses, correlating a sampled sequence representative of the received coded pulse against a sampled representation of each of a plurality of cyclically shifted versions of a code sequence, to determine the cyclically shifted version of the code sequence corresponding to the pulse. Estimating the code phase for each coded pulse in these implementations may comprise estimating the code phase based on a timing derived from the correlation peak for the correlation of the sampled sequence against the cyclically shifted version of the code sequence corresponding to the pulse. In some implementations, a covering pseudorandom (PN) sequence may have been applied to the coded pulse – in these implementations, the method may comprise removing the covering pseudorandom sequence from samples of the received coded pulse, to obtain the sampled sequence representative of the received coded pulse, prior to performing the correlation. Equivalently, of course, the correlation can be performed with PN-covered versions of the code sequence, thus obviating the need to remove the PN covering from the received signal.

As shown at block 1330, the method then proceeds with the step of using the estimated code phases for coded pulses detected on a first channel of the second set to estimate the sum of

(a) frequency deviation in the received signal arising from Doppler shift and (b) frequency deviation in the received signal arising from reference frequency error in either or both of the radio receiver and the transmitter of the received radio signal. An example of this was discussed above, where Channel 19 of the Link 16 was used as this first channel. More generally, any channel may be used. Advantageously, the receiver converts this channel all the way to baseband before carrying out the step shown in block 1330, so that the term involving the initial TOA estimate in Equation (9) becomes zero. This may be done, for example, by down-converting the radio signal using direct down-conversion with a local frequency source having a frequency nominally equal to the channel frequency of the first channel.

In some implementations, estimating the sum of (a) frequency deviation in the received signal arising from Doppler shift and (b) frequency deviation in the received signal arising from reference frequency error in either or both of the radio receiver and the transmitter of the received radio signal may comprise determining a rate of change versus time in estimated code phases for the coded pulses detected on the first channel and calculating the estimated sum from the determined rate of change.

As shown at block 1340, the method further comprises, for each channel of the second set, calculating corrected code phases for each of the estimated code phases corresponding to the channel, based on the estimated sum of frequency deviations, and averaging the corrected code phases for the channel to generate an average code phase for the channel. Then, as shown at block 1350, the method comprises calculating a first TOA error estimate, based on the average code phase for the first channel, the first TOA error estimate representing an estimate of error in the estimated coarse TOA. Calculating corrected code phases for each of the estimated code phases may comprise, for example, subtracting, from the estimated code phase, a term proportional to the estimated sum of the frequency deviations, the channel frequency corresponding to the received coded pulse, and a pulse interval.

As shown at block 1360, the method comprises calculating a refined TOA error estimate, based on the average code phase for a second channel of the second set, the first TOA error estimate, the estimated sum of frequency deviations, and the channel frequency or channel frequency offset of the second channel. Advantageously, the second channel of the second set is a closest channel of the second set to the first channel, in frequency. As shown at block 1370, the method still further comprises calculating one or more further refined TOA error

estimates, wherein each further refined TOA error estimate is based on the most recently calculated refined TOA error estimate or further refined TOA estimate, the average code phase for one of the remaining channels of the second set, the estimated sum of the frequency deviations, and the channel frequency or channel frequency offset of the one of the remaining channels. This calculating of the one or more further refined TOA error estimates may comprise, for example, selecting channels for this iterative calculating in order of closeness, in frequency, of the selected channels to the first channel.

The steps shown at block 1360 and 1370 comprise the iterative process described above for refining the TOA error estimate. Thus, in these steps, the TOA estimate is refined and phase wrap-around ambiguities are resolved and removed. Note that the terms "refined TOA error estimate" and "further refined TOA estimate," as used herein, should be understood to refer to either an update of a calculated error in the initial TOA or an update of the TOA estimate itself, as these are functionally equivalent.

The output of the method shown in Figure 13 is a high-precision TOA estimate (or, equivalently, an initial TOA estimate and a precision estimate of the error in the initial TOA estimate). This refined TOA estimate can be used to estimate a distance or propagation delay between the radio receiver and the transmitter of the received radio signal, as shown at block 1380 of Figure 13. This estimated distance or propagation delay can be used, in turn, to estimate a location for the radio receiver or the transmitter of the received signal, as shown at block 1390 of Figure 13, using any of a variety of well-known triangulation techniques.

Figure 14 is a block diagram presenting a simplified view of a radio receiver 1400, which might be as a Link 16 radio receiver for example, configured to carry out one or more of the techniques described herein, including any one or more of the variations of the method shown in Figure 13. Thus, the illustrated radio receiver 1400 is, generally speaking configured to determine TOA, at the radio receiver 1400, of a radio signal transmitted in the form of a series of coded pulses on each of a plurality of radio channels having distinct channel frequencies. As discussed above, the code phases of the coded pulses in the radio signal as transmitted are coherently related across time and across the plurality of radio channels.

As seen in the figure, radio receiver 1400 comprises radio circuitry 1410, which is configured to down-convert the radio signal received via antenna 1450. Radio receiver 1400 further comprises signal processing circuitry 1420, which is operatively coupled to the radio circuitry

1410. Signal processing circuitry 1420 is configured to carry out a method according any of the methods described herein, including any of those illustrated in Figure 13. Thus, the signal processing circuitry 1420 may be configured to estimate a coarse TOA for the received radio signal, by detecting preamble sequences in each channel of a first set of the channels, non-coherently combining the detected preamble sequences, and estimating timing for a peak resulting from the non-coherent combining.

Signal processing circuitry 1420 may be further configured to perform symbol detection for each of a plurality of the coded pulses, on each channel of a second set of the channels, and estimate a code phase for each of the coded pulses, based on the symbol detection. Signal processing circuitry 1420 may be further configured to, based on the estimated code phases for coded pulses detected on a first channel of the second set, estimate the sum of (a) frequency deviation in the received signal arising from Doppler shift and (b) frequency deviation in the received signal arising from reference frequency error in either or both of the radio receiver and the transmitter of the received radio signal, and, for each channel of the second set, calculate corrected code phases for each of the estimated code phases corresponding to the channel, based on the estimated sum of frequency deviations, and average the corrected code phases for the channel to generate an average code phase for the channel. Signal processing circuit 1420 may be still further configured to calculate a first TOA error estimate, based on the average code phase for the first channel, the first TOA error estimate representing an estimate of error in the estimated coarse TOA, and to calculate a refined TOA error estimate, based on the average code phase for a second channel of the second set, the first TOA error estimate, the estimated sum of frequency deviations, and the channel frequency or channel frequency offset of the second channel. Signal processing circuit 1420 may yet further be configured to calculate one or more further refined TOA error estimates, wherein each further refined TOA error estimate is based on the most recently calculated refined TOA error estimate or further refined TOA estimate, the average code phase for one of the remaining channels of the second set, the estimated sum of the frequency deviations, and the channel frequency or channel frequency offset of the one of the remaining channels.

In some embodiments of radio receiver 1400, the coded pulses may be cyclic code-shift keying (CCSK) -coded pulses. In these embodiments, the signal processing circuitry 1420 may be configured to perform symbol detection for each of the plurality of coded pulses by,

for each of the coded pulses, correlating a sampled sequence representative of the received coded pulse against a sampled representation of each of a plurality of cyclically shifted versions of a code sequence, to determine the cyclically shifted version of the code sequence corresponding to the pulse. The signal processing circuitry 1420 may be further configured to estimate the code phase for each coded pulse by estimating the code phase based on a timing derived from the correlation peak for the correlation of the sampled sequence against the cyclically shifted version of the code sequence corresponding to the pulse. In at least some of these embodiments, the signal processing circuitry 1420 may be further configured to remove a covering pseudorandom sequence from samples of the received coded pulse, to obtain the sampled sequence representative of the received coded pulse.

In some embodiments, the signal processing circuitry 1420 may be configured to estimate the sum of (a) frequency deviation in the received signal arising from Doppler shift and (b) frequency deviation in the received signal arising from reference frequency error in either or both of the radio receiver and the transmitter of the received radio signal by determining a rate of change versus time in estimated code phases for the coded pulses detected on the first channel and calculating the estimated sum from the determined rate of change.

In some embodiments, signal processing circuitry 1420 may be configured to calculate corrected code phases for each of the estimated code phases by subtracting, from the estimated code phase, a term proportional to the estimated sum of the frequency deviations, the channel frequency corresponding to the received coded pulse, and a pulse interval.

In some embodiments, radio circuitry 1410 may be configured to down-convert the radio signal using direct down-conversion with a local frequency source, e.g., a local oscillator 1425, having a frequency nominally equal to the channel frequency of the first channel. In some of these embodiments, the second channel of the second set may be a closest channel of the second set to the first channel, in frequency. Further, the signal processing circuitry may be configured to select channels for calculating the one or more further refined TOA error estimates in order of closeness, in frequency, of the selected channels to the first channel.

In some embodiments, signal processing circuitry 1420 is further configured to estimate a distance or propagation delay between the radio receiver and the transmitter of the received radio signal, based on a final one of the refined TOA estimates. Likewise, the signal processing circuitry 1420 may be further configured to estimate a location for the radio

receiver or the transmitter of the received radio signal, based on the estimated distance or propagation delay.

Radio circuitry 1410 may comprise any of a wide variety of radio architectures, and may comprise combinations of any one or more of low-noise amplifiers, mixers, local oscillators (such as local oscillator 1425 shown in Figure 14), reference clock oscillators (such as reference clock 1415 in Figure 14, which is tied to crystal oscillator 1417), radio-frequency switches, filters, isolators, and analog-to-digital converters. Signal processing circuitry 1420 may comprise digital logic implemented in any of various forms, including one or more field-programmable gate arrays (FPGAs) and/or application-specific integrated circuits (ASICs), or the like. Signal processing circuitry 1420 may comprise one or more digital processors, including one or more digital-signal processors (DSPs), reduced instruction set computers (RISCs), and/or general-purpose or specialty microprocessors or microcontrollers. Radio receiver 1400 may further comprise, in various embodiments, a battery 1430, power supply circuitry 1440, and a system controller circuit 1460 configured to control the overall operation of radio receiver 1400.

Notably, modifications and other embodiments of the disclosed invention(s) will come to mind to one skilled in the art having the benefit of the teachings presented in the foregoing descriptions and the associated drawings. Therefore, it is to be understood that the invention(s) is/are not to be limited to the specific embodiments disclosed and that modifications and other embodiments are intended to be included within the scope of this disclosure. Although specific terms may be employed herein, they are used in a generic and descriptive sense only and not for purposes of limitation.

CLAIMS

What is claimed is:

- 1. A method, in a radio receiver, for determining time-of-arrival (TOA), at the radio receiver of a radio signal transmitted in the form of a series of coded pulses on each of a plurality of radio channels having distinct channel frequencies, the method comprising:
 - estimating a coarse TOA for the received radio signal, by detecting preamble sequences in each channel of a first set of the channels, non-coherently combining the detected preamble sequences, and estimating timing for a peak resulting from the non-coherent combining;
 - performing symbol detection for each of a plurality of the coded pulses, on each channel of a second set of the channels, and estimating a code phase for each of the coded pulses, based on the symbol detection;
 - based on the estimated code phases for coded pulses detected on a first channel of the second set, estimating the sum of (a) frequency deviation in the received signal arising from Doppler shift and (b) frequency deviation in the received signal arising from reference frequency error in either or both of the radio receiver and the transmitter of the received radio signal;
 - for each channel of the second set, calculating corrected code phases for each of the estimated code phases corresponding to the channel, based on the estimated sum of frequency deviations, and averaging the corrected code phases for the channel to generate an average code phase for the channel;
 - calculating a first TOA error estimate, based on the average code phase for the first channel, the first TOA error estimate representing an estimate of error in the estimated coarse TOA;
 - calculating a refined TOA error estimate, based on the average code phase for a second channel of the second set, the first TOA error estimate, the estimated sum of frequency deviations, and the channel frequency or channel frequency offset of the second channel; and
 - calculating one or more further refined TOA error estimates, wherein each further refined TOA error estimate is based on the most recently calculated refined TOA error estimate or further refined TOA estimate, the average code phase for one of the remaining channels of the second set, the estimated sum of the frequency deviations, and the channel frequency or channel frequency offset

of the one of the remaining channels.

2. The method of claim 1, wherein the code phases of the coded pulses in the radio signal as transmitted are coherently related across time and across the plurality of radio channels.

3. The method of claim 1 or 2, wherein:

the coded pulses are cyclic code-shift keying (CCSK) -coded pulses;

performing symbol detection for each of the plurality of coded pulses comprises, for

each of the coded pulses, correlating a sampled sequence representative of the
received coded pulse against a sampled representation of each of a plurality of
cyclically shifted versions of a code sequence, to determine the cyclically
shifted version of the code sequence corresponding to the pulse; and
estimating the code phase for each coded pulse comprises estimating the code phase
based on a timing derived from the correlation peak for the correlation of the
sampled sequence against the cyclically shifted version of the code sequence
corresponding to the pulse.

- 4. The method of claim 3, wherein the method comprises removing a covering pseudorandom sequence from samples of the received coded pulse, to obtain the sampled sequence representative of the received coded pulse.
- 5. The method of any one of claims 1-4, wherein estimating the sum of (a) frequency deviation in the received signal arising from Doppler shift and (b) frequency deviation in the received signal arising from reference frequency error in either or both of the radio receiver and the transmitter of the received radio signal comprises:

determining a rate of change versus time in estimated code phases for the coded pulses detected on the first channel; and calculating the estimated sum from the determined rate of change.

6. The method of any one of claims 1-5, wherein calculating corrected code phases for each of the estimated code phases comprises subtracting, from the estimated code phase, a term proportional to the estimated sum of the frequency deviations, the channel frequency corresponding to the received coded pulse, and a pulse interval.

7. The method of any one of claims 1-6, wherein the method comprises down-converting the radio signal using direct down-conversion with a local frequency source having a frequency nominally equal to the channel frequency of the first channel.

- 8. The method of claim 7, wherein the second channel of the second set is a closest channel of the second set to the first channel, in frequency.
- 9. The method of claim 8, wherein calculating the one or more further refined TOA error estimates comprises, selecting channels for said calculating in order of closeness, in frequency, of the selected channels to the first channel.
- 10. The method of any one of claims 1-9, wherein the radio signal is a Tactical Data Link signal.
- 11. The method of any one of claims 1-10, wherein the method further comprises:
 estimating a distance or propagation delay between the radio receiver and the
 transmitter of the received radio signal, based on a final one of the refined
 TOA estimates.
- 12. The method of claim 11, further comprising estimating a location for the radio receiver or the transmitter of the received radio signal, based on the estimated distance or propagation delay.
- 13. A radio receiver for determining time-of-arrival (TOA), at the radio receiver, of a radio signal transmitted in the form of a series of coded pulses on each of a plurality of radio channels having distinct channel frequencies, the radio receiver comprising:

radio circuitry configured to down-convert the received radio signal; and signal processing circuitry operatively coupled to the radio circuitry and configured to:

estimate a coarse TOA for the received radio signal, by detecting preamble sequences in each channel of a first set of the channels, non-coherently combining the detected preamble sequences, and estimating timing for a peak resulting from the non-coherent combining;

perform symbol detection for each of a plurality of the coded pulses, on each

channel of a second set of the channels, and estimate a code phase for each of the coded pulses, based on the symbol detection;

- based on the estimated code phases for coded pulses detected on a first channel of the second set, estimate the sum of (a) frequency deviation in the received signal arising from Doppler shift and (b) frequency deviation in the received signal arising from reference frequency error in either or both of the radio receiver and the transmitter of the received radio signal;
- for each channel of the second set, calculate corrected code phases for each of the estimated code phases corresponding to the channel, based on the estimated sum of frequency deviations, and average the corrected code phases for the channel to generate an average code phase for the channel;
- calculate a first TOA error estimate, based on the average code phase for the first channel, the first TOA error estimate representing an estimate of error in the estimated coarse TOA;
- calculate a refined TOA error estimate, based on the average code phase for a second channel of the second set, the first TOA error estimate, the estimated sum of frequency deviations, and the channel frequency or channel frequency offset of the second channel; and
- calculate one or more further refined TOA error estimates, wherein each further refined TOA error estimate is based on the most recently calculated refined TOA error estimate or further refined TOA estimate, the average code phase for one of the remaining channels of the second set, the estimated sum of the frequency deviations, and the channel frequency or channel frequency offset of the one of the remaining channels.
- 14. The radio receiver of claim 13, wherein the code phases of the coded pulses in the radio signal as transmitted are coherently related across time and across the plurality of radio channels.
- 15. The radio receiver of claim 13 or 14, wherein the coded pulses are cyclic code-shift keying (CCSK) -coded pulses, and wherein the signal processing circuitry is configured to:

perform symbol detection for each of the plurality of coded pulses by, for each of the coded pulses, correlating a sampled sequence representative of the received coded pulse against a sampled representation of each of a plurality of cyclically shifted versions of a code sequence, to determine the cyclically shifted version of the code sequence corresponding to the pulse, and estimate the code phase for each coded pulse by estimating the code phase based on a timing derived from the correlation peak for the correlation of the sampled sequence against the cyclically shifted version of the code sequence corresponding to the pulse.

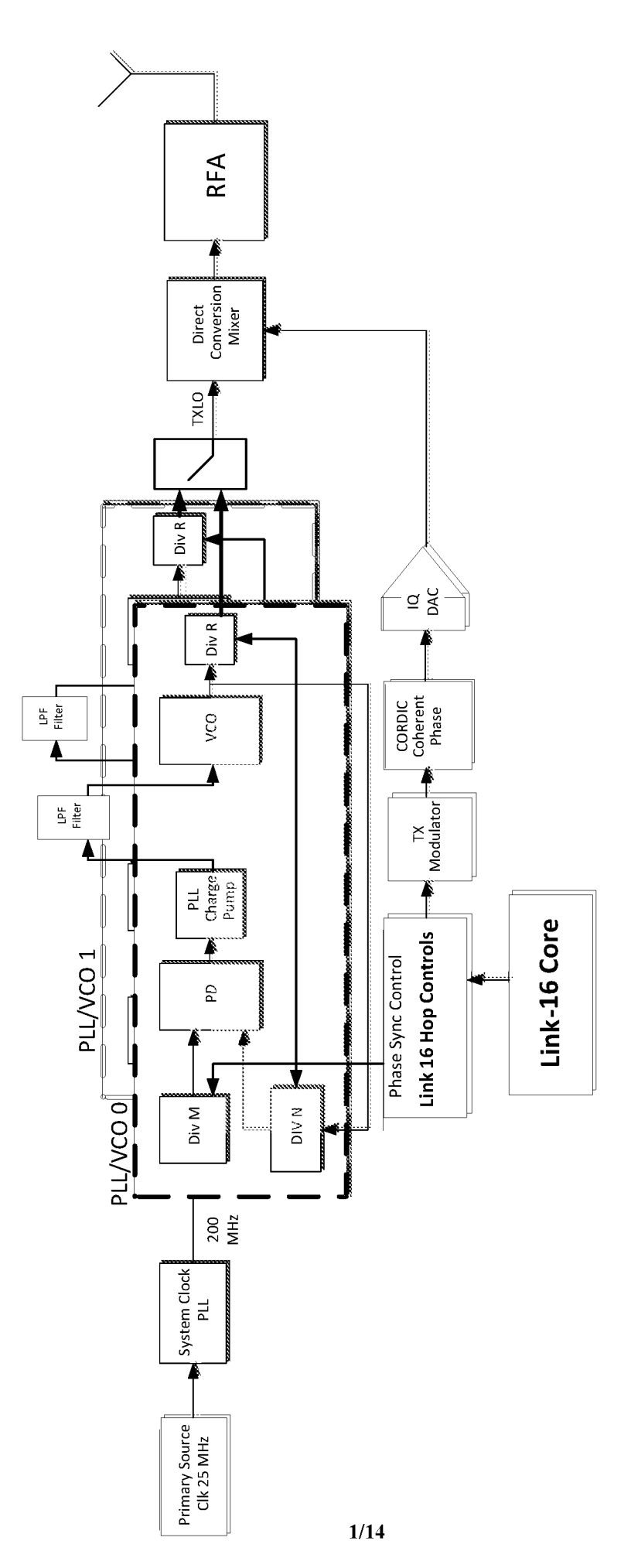
- 16. The radio receiver of claim 15, wherein the signal processing circuitry is configured to remove a covering pseudorandom sequence from samples of the received coded pulse, to obtain the sampled sequence representative of the received coded pulse.
- 17. The radio receiver of any one of claims 13-16, wherein the signal processing circuitry is configured to estimate the sum of (a) frequency deviation in the received signal arising from Doppler shift and (b) frequency deviation in the received signal arising from reference frequency error in either or both of the radio receiver and the transmitter of the received radio signal by:

determining a rate of change versus time in estimated code phases for the coded pulses detected on the first channel; and calculating the estimated sum from the determined rate of change.

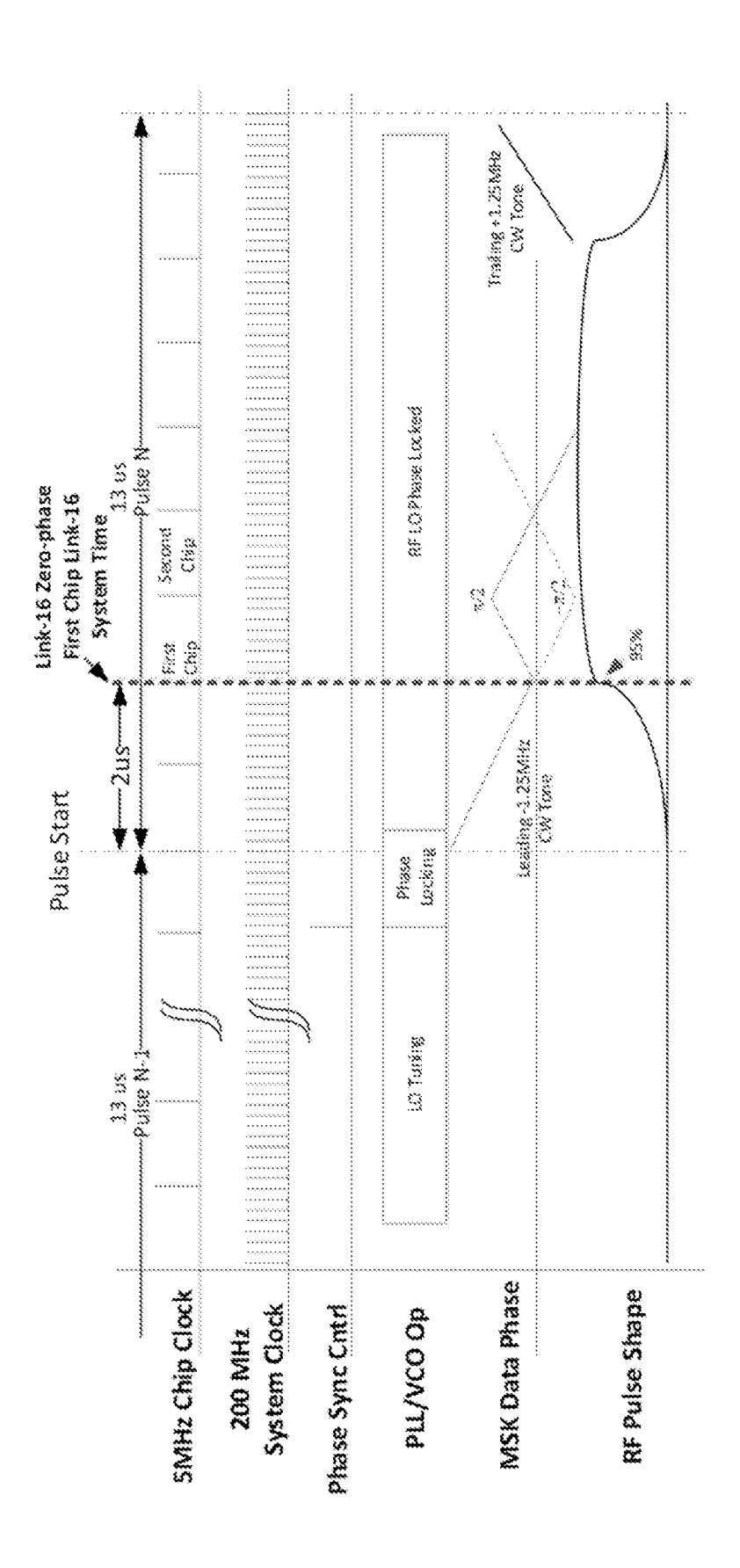
- 18. The radio receiver of any one of claims 13-17, wherein the signal processing circuitry is configured to calculate corrected code phases for each of the estimated code phases by subtracting, from the estimated code phase, a term proportional to the estimated sum of the frequency deviations, the channel frequency corresponding to the received coded pulse, and a pulse interval.
- 19. The radio receiver of any one of claims 13-18, wherein the radio circuitry is configured to down-convert the radio signal using direct down-conversion with a local frequency source having a frequency nominally equal to the channel frequency of the first channel.

20. The radio receiver of claim 19, wherein the second channel of the second set is a closest channel of the second set to the first channel, in frequency.

- 21. The radio receiver of claim 20, wherein the signal processing circuitry is configured to select channels for calculating the one or more further refined TOA error estimates in order of closeness, in frequency, of the selected channels to the first channel.
- 22. The radio receiver of any one of claims 13-21, wherein the radio signal is a Tactical Data Link signal.
- 23. The radio receiver of any one of claims 13-22, wherein the signal processing circuitry is further configured to estimate a distance or propagation delay between the radio receiver and the transmitter of the received radio signal, based on a final one of the refined TOA estimates.
- 24. The radio receiver of claim 23, wherein the signal processing circuitry is further configured to estimate a location for the radio receiver or the transmitter of the received radio signal, based on the estimated distance or propagation delay.



Fia. 1



-ia. 2

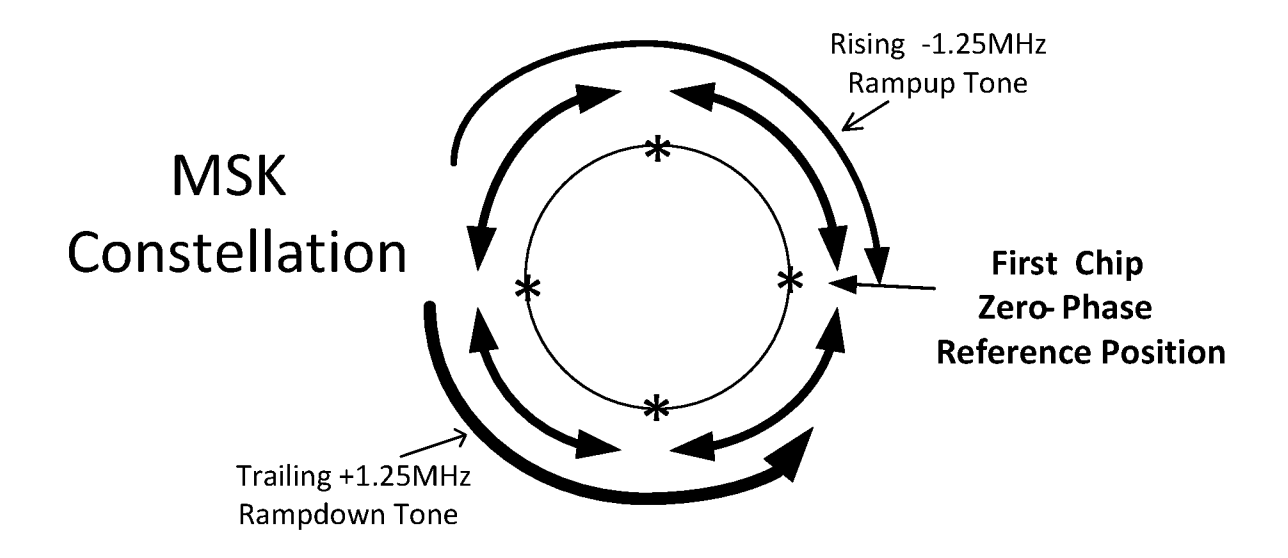
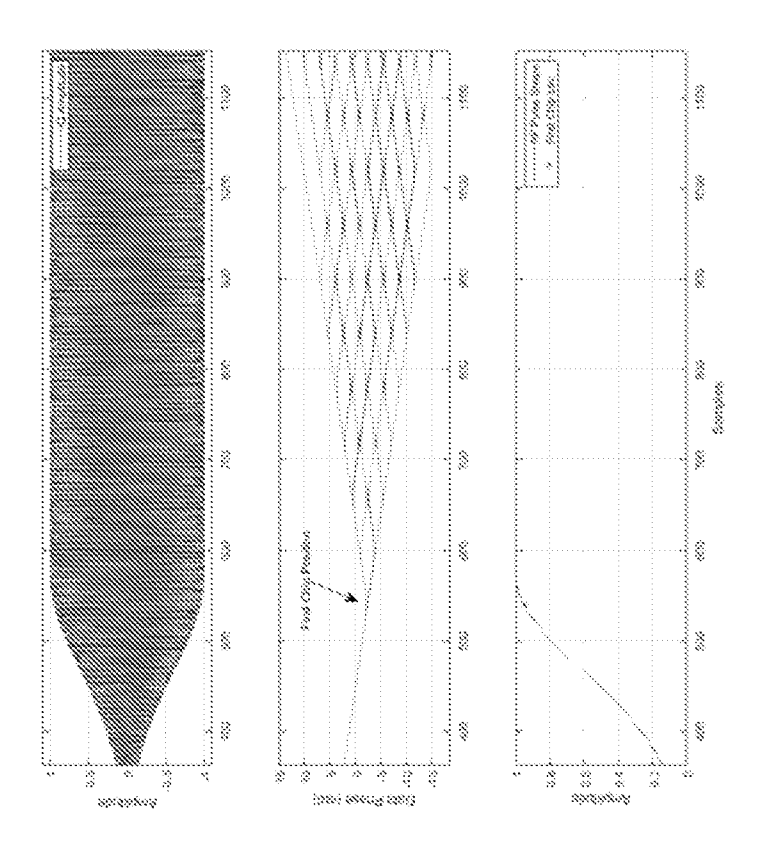
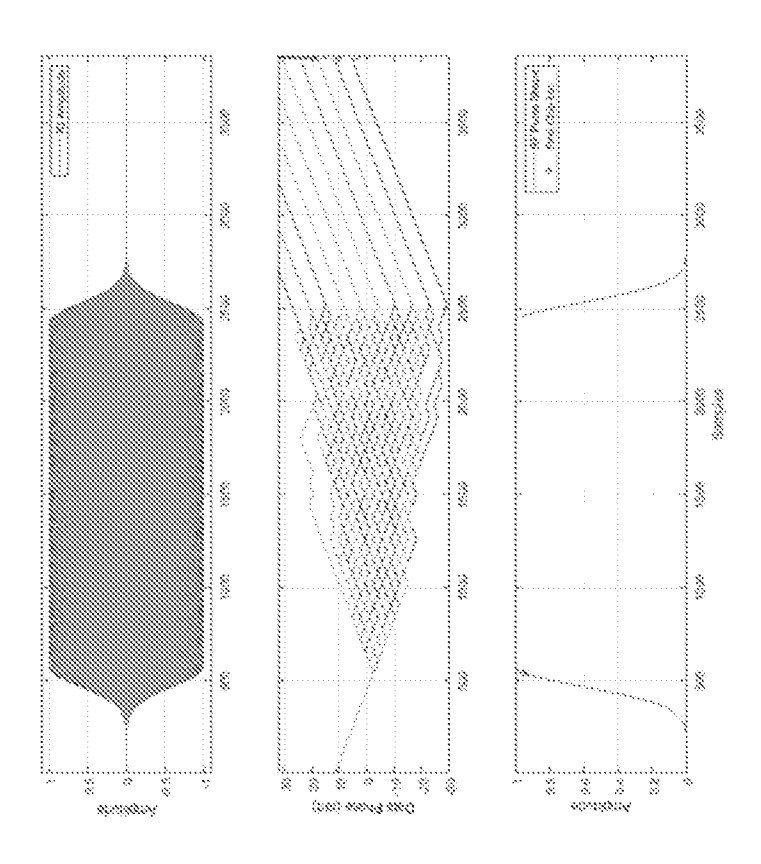


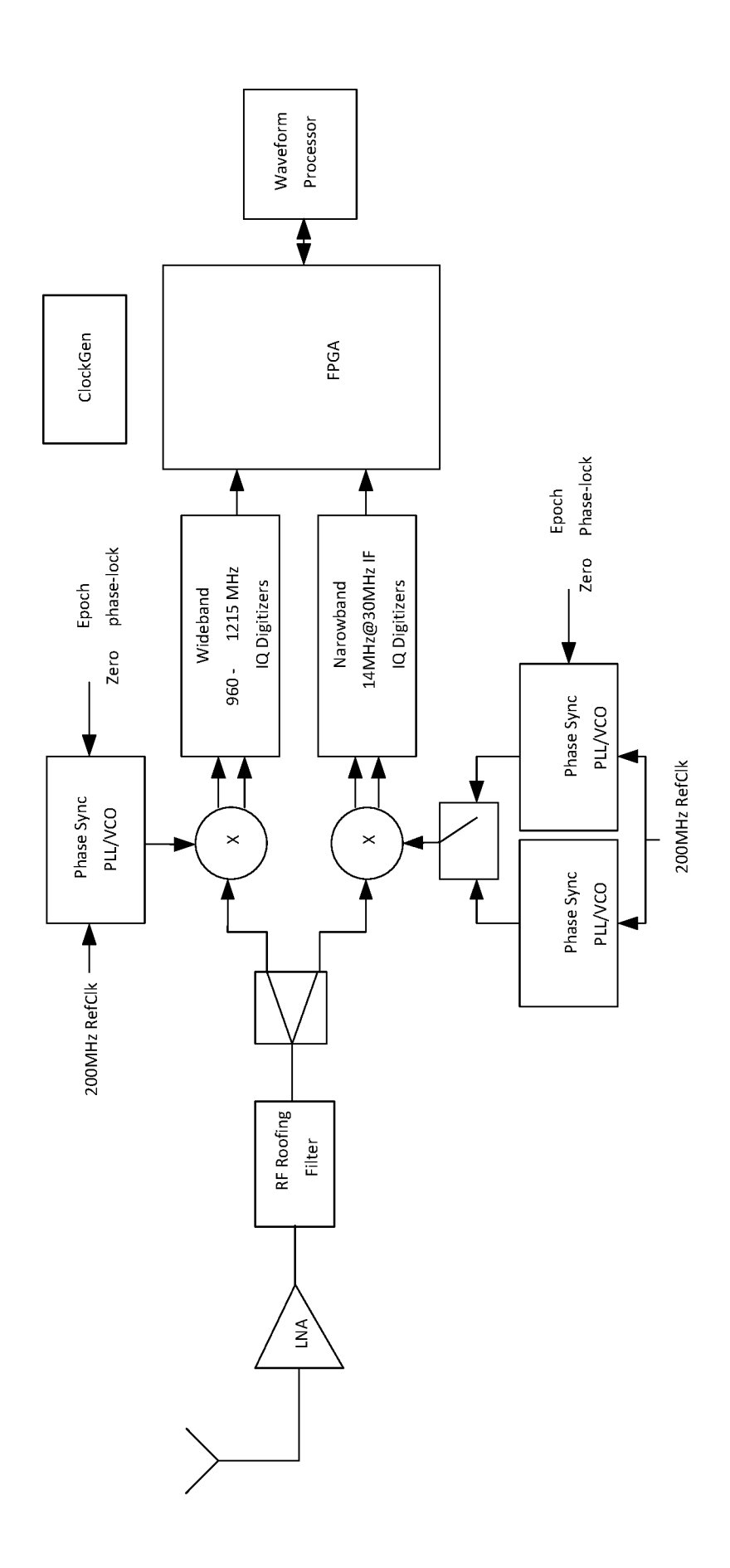
Fig. 3

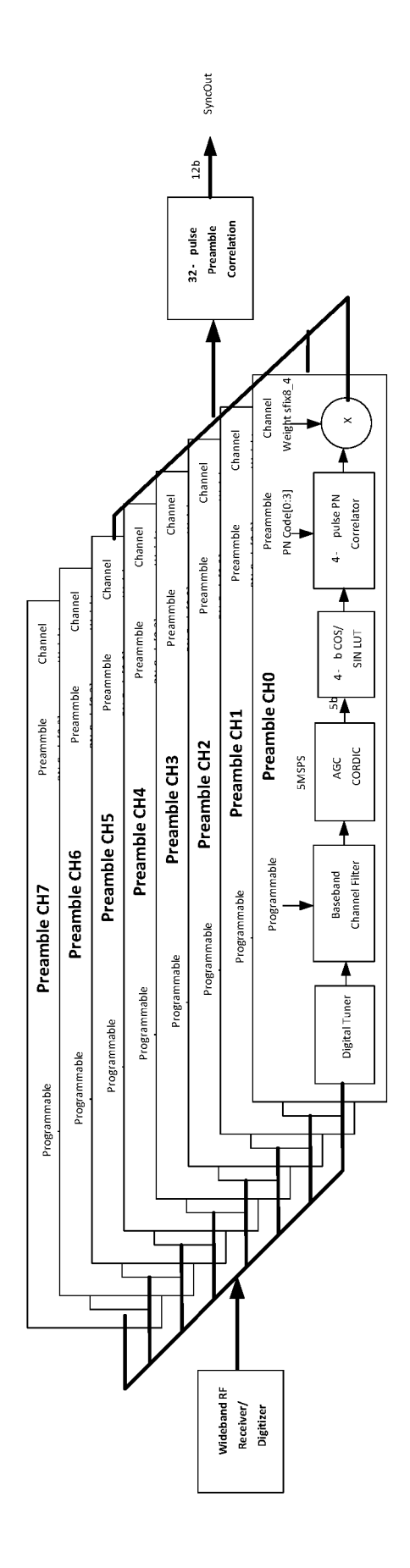




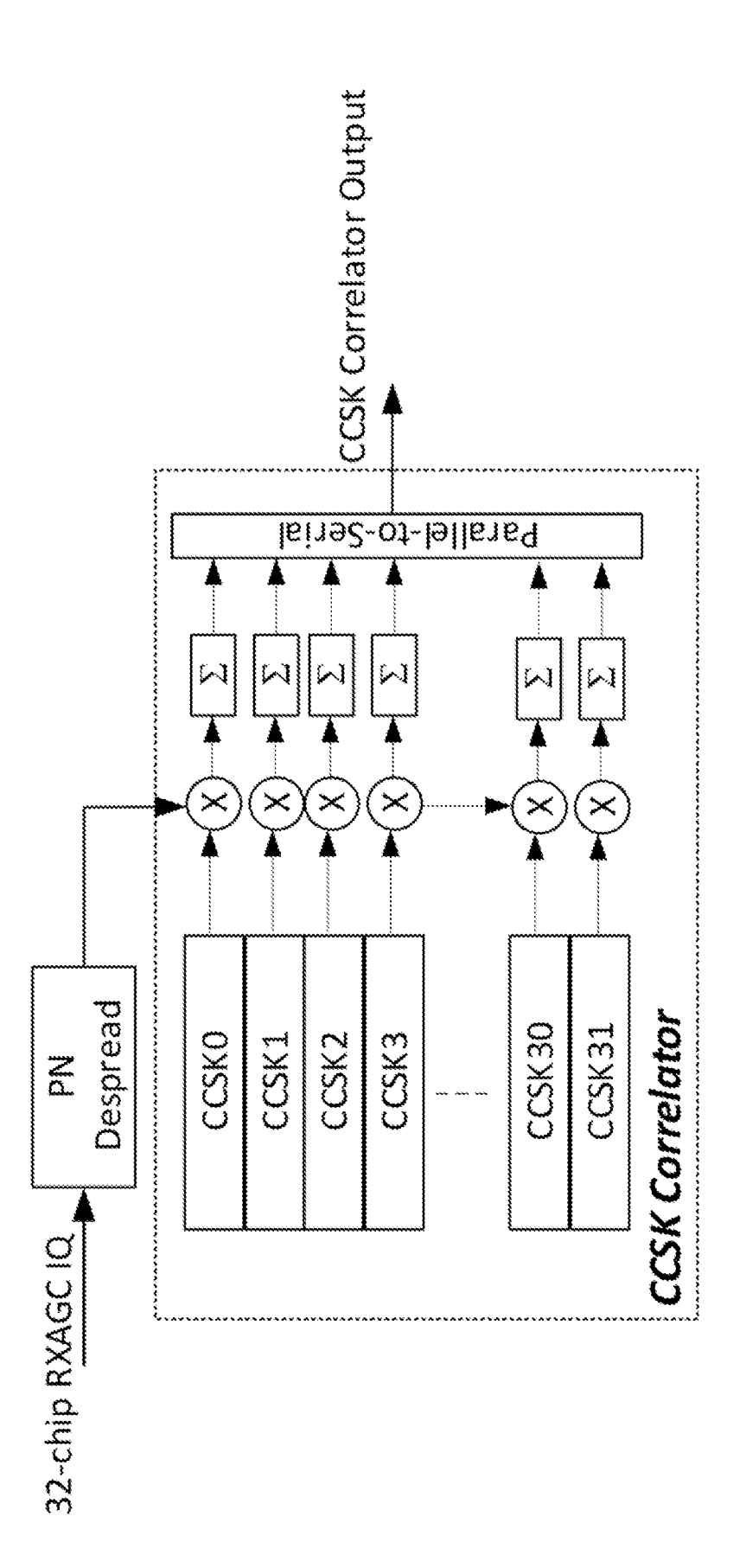








Fia. 6



Fia. 7

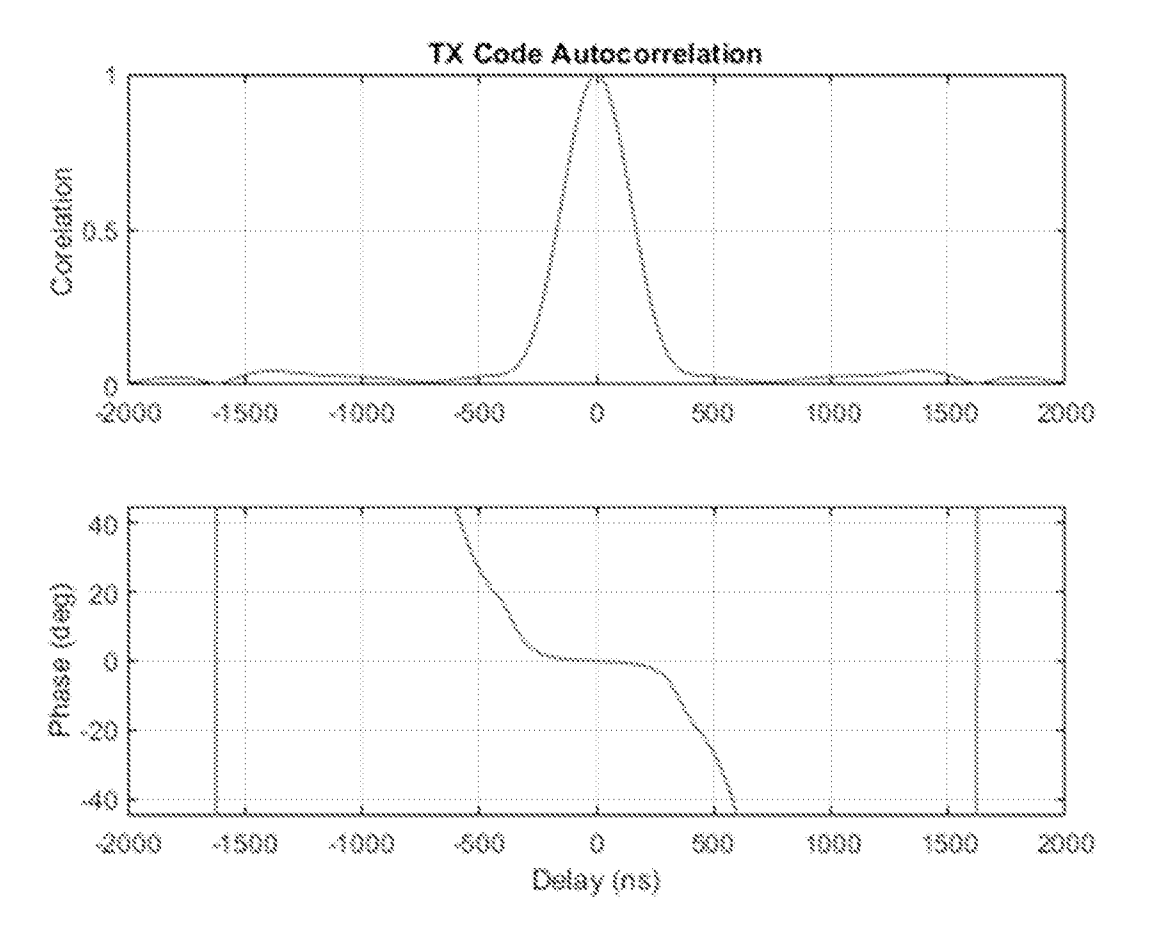
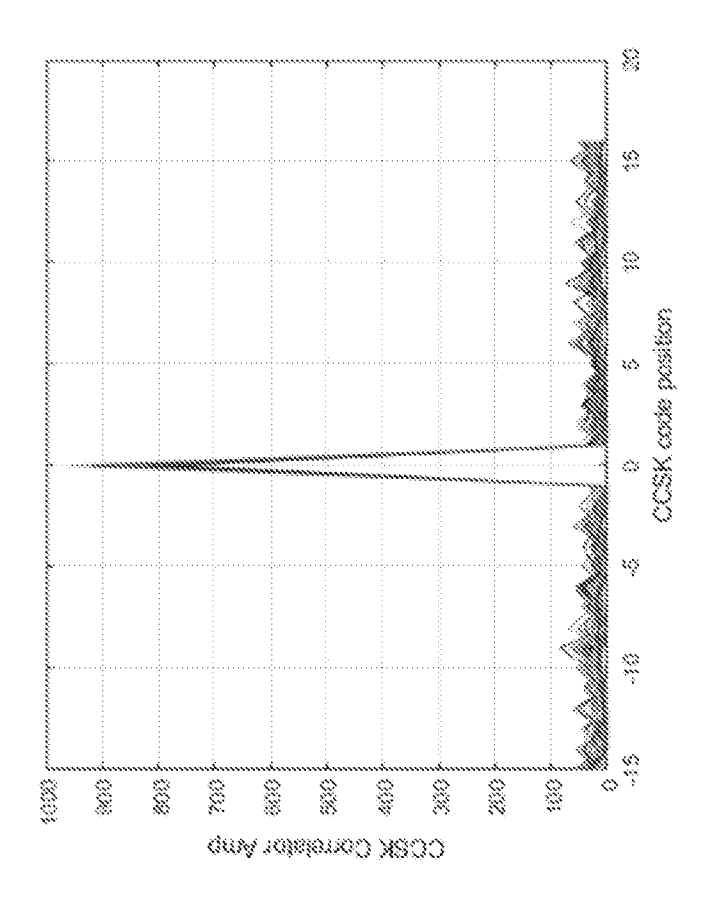
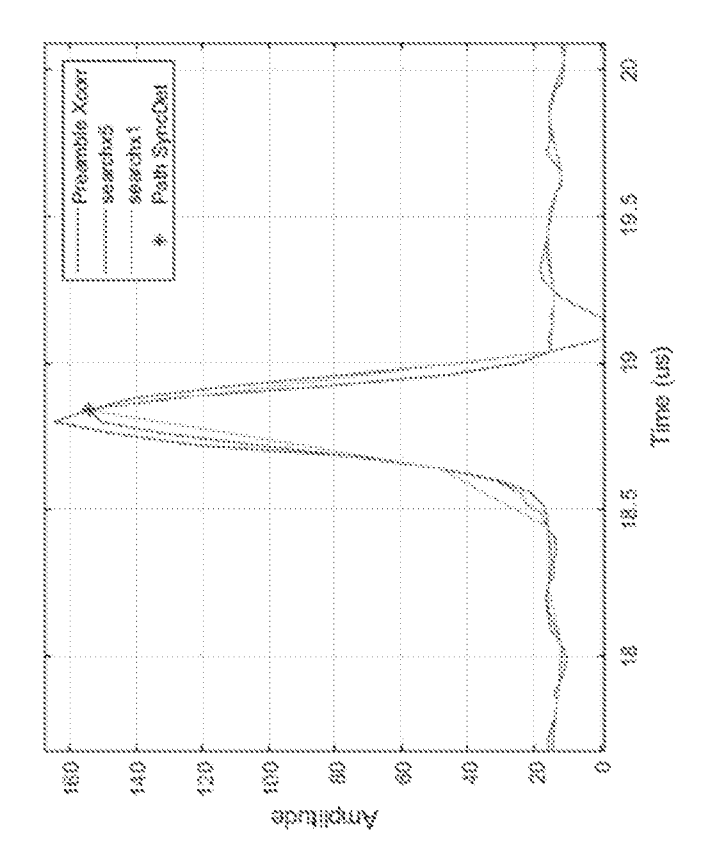
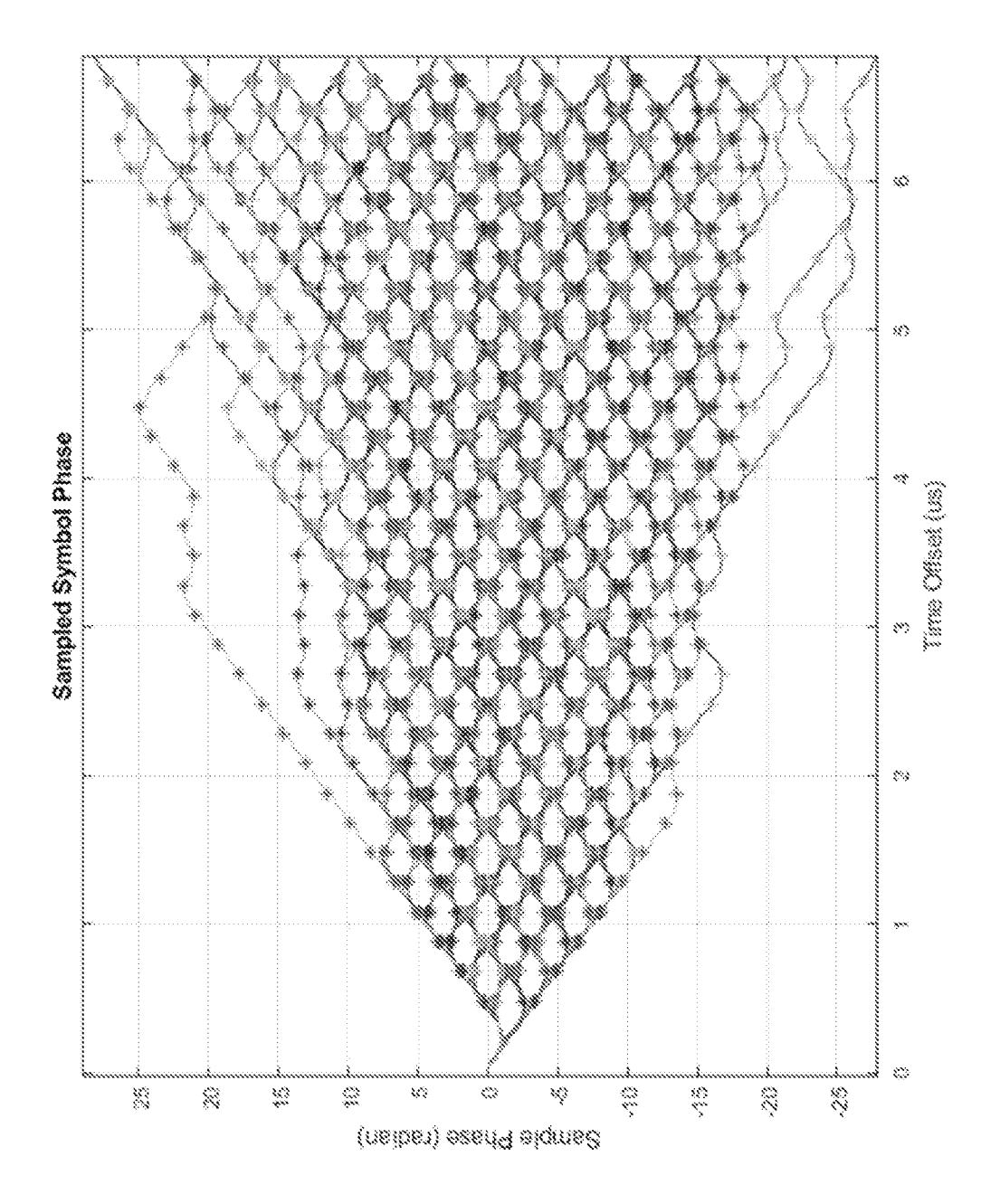


Fig. 8









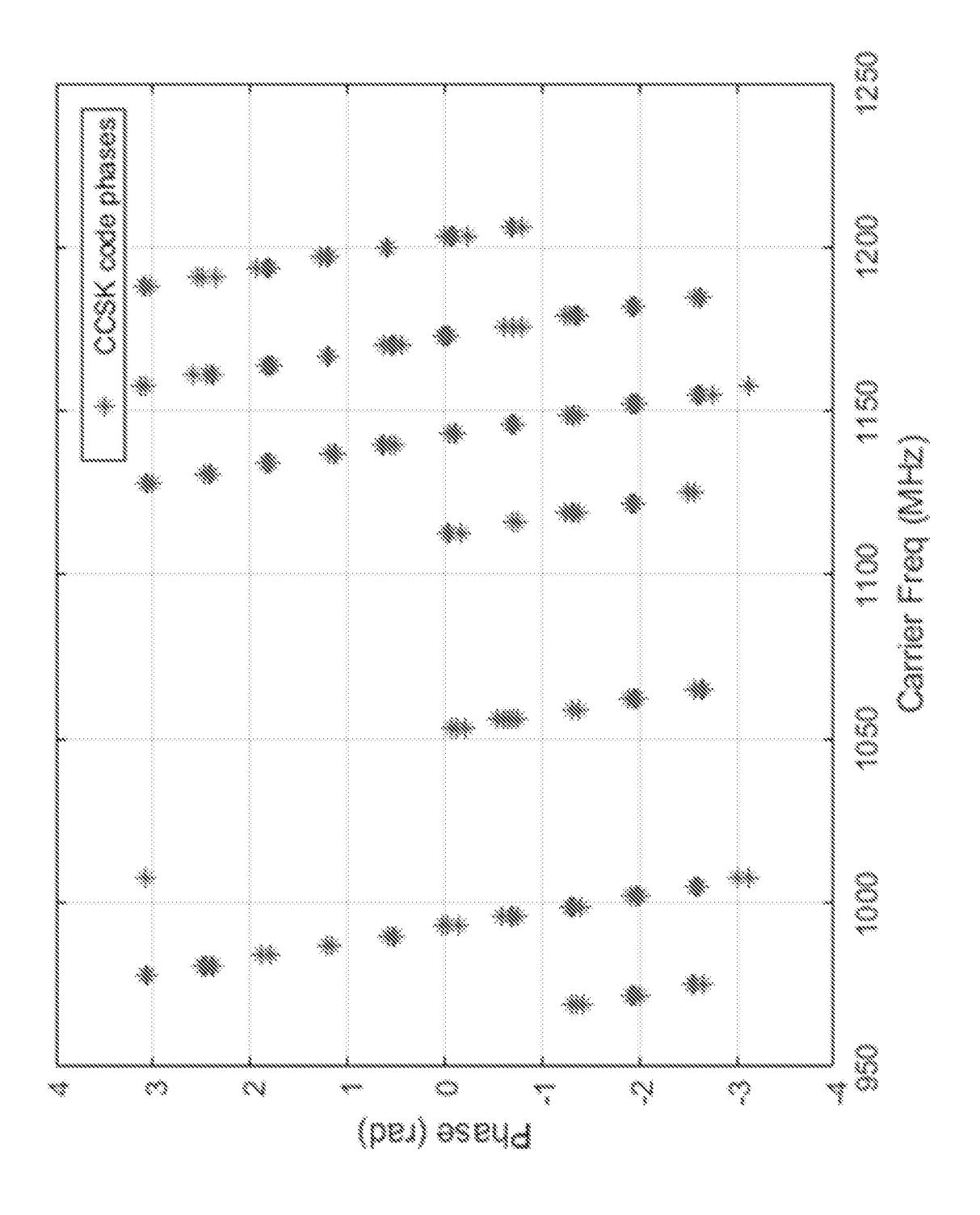
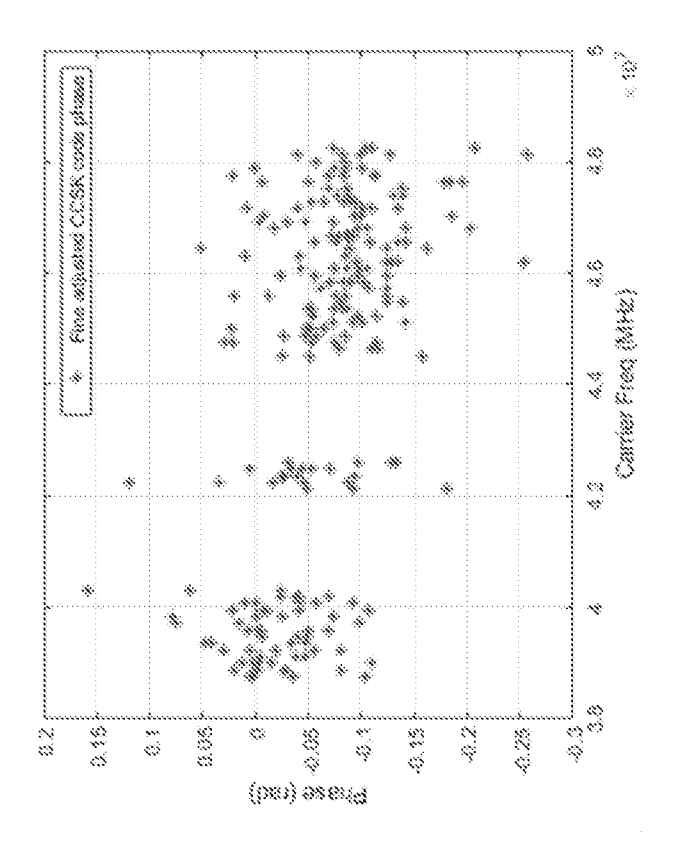
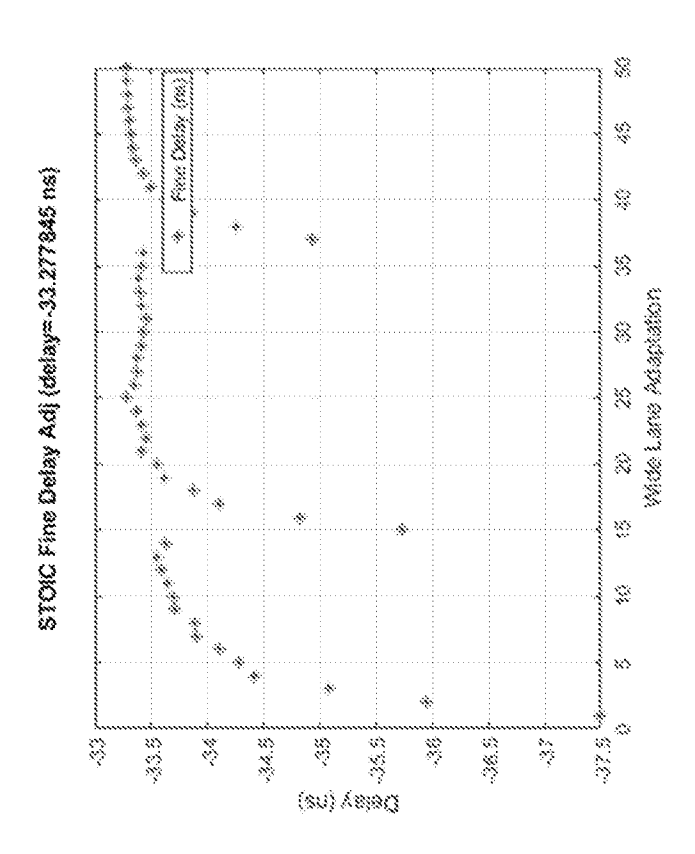


Fig. 11

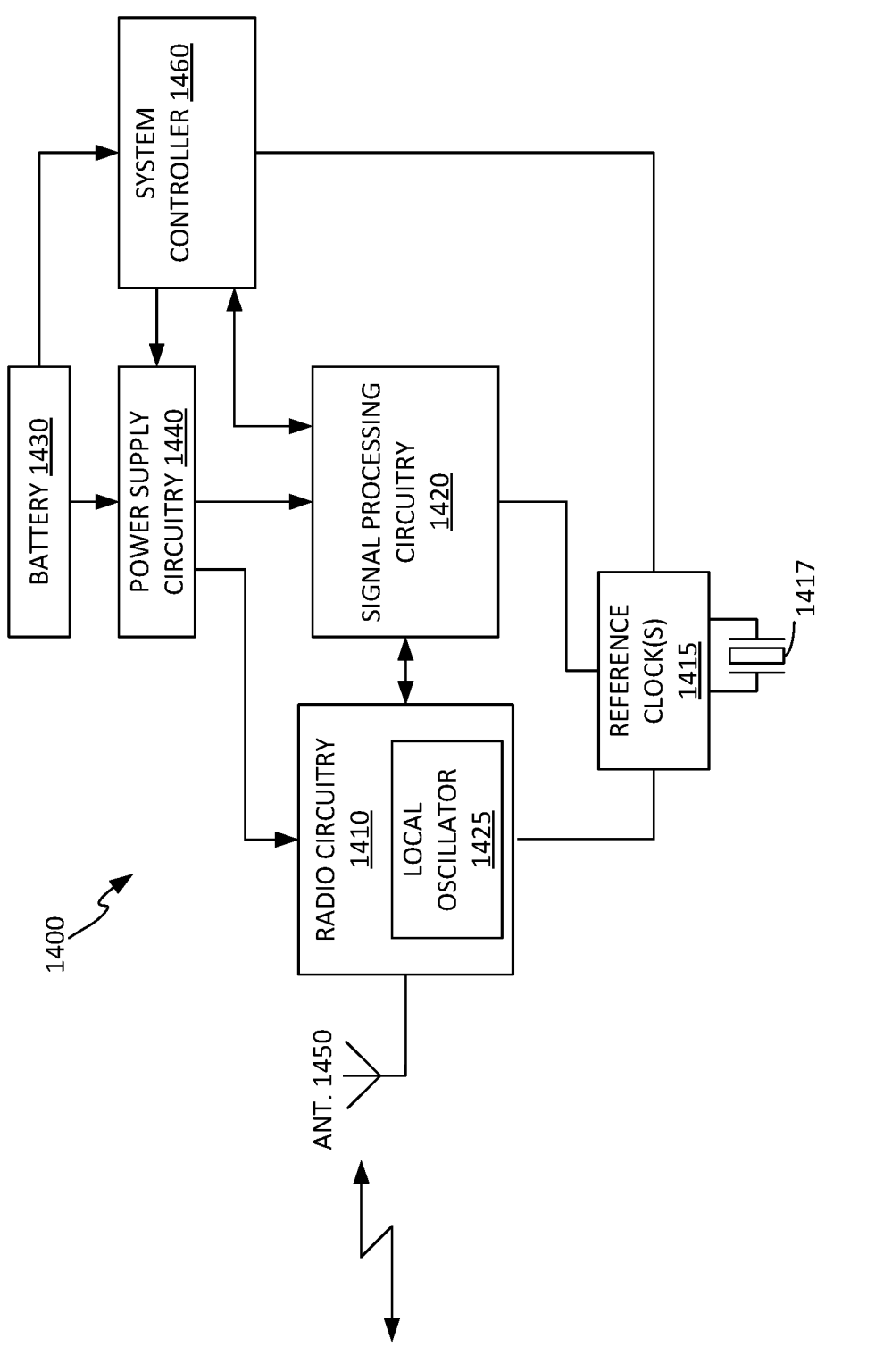




ESTIMATE COARSE TOA FOR RECEIVED RADIO SIGNAL, BY DETECTING PREAMBLE SEQUENCES, NON-COHERENTLY COMBINING, AND ESTIMATING TIMING FOR A PEAK RESULTING FROM THE NON-**COHERENT COMBINING** 1310 PERFORM SYMBOL DETECTION FOR EACH OF A PLURALITY OF CODED PULSES, ON EACH CHANNEL OF SECOND SET OF CHANNELS, AND ESTIMATE A CODE PHASE FOR EACH CODED PULSE 1320 BASED ON ESTIMATED CODE PHASES, ESTIMATE SUM OF (A) FREQUENCY DEVIATION FROM DOPPLER SHIFT AND (B) FREQUENCY DEVIATION FROM REFERENCE FREQUENCY ERROR(S) 1330 FOR EACH CHANNEL IN SECOND SET, CALCULATE CORRECTED CODE PHASES AND AVERAGE CORRECTED CODE PHASES, TO GENERATE AVERAGE CODE PHASE FOR CHANNEL 1340 CALCULATE FIRST TOA ERROR ESTIMATE, BASED ON AVERAGE CODE PHASE FOR FIRST CHANNEL IN **SECOND SET** 1350 CALCULATE REFINED TOA ERROR ESTIMATE, BASED ON AVERAGE CODE PHASE FOR SECOND CHANNEL OF SECOND SET, THE FIRST TOA ERROR ESTIMATE, THE ESTIMATED SUM OF FREQUENCY DEVIATIONS, AND FREQUENCY OR FREQUENCY OFFSET OF SECOND CHANNEL 1360 CALCULATE ONE OR MORE FURTHER REFINED TOA ESTIMATES, EACH BASED ON MOST RECENTLY CALCULATED ESTIMATE, THE AVERAGE CODE PHASE FOR A CHANNEL OF THE SECOND SET, THE ESTIMATED SUM OF FREQUENCY DEVIATIONS, AND FREQUENCY OR FREQUENCY OFFSET OF CHANNEL 1370 ESTIMATE DISTANCE OR PROPAGATION DELAY, BASED ON FINAL ESTIMATE OF TOA/TOA ERROR 1380

Fig. 13

ESTIMATE LOCATION FOR RADIO RECEIVER OR TRANSMITTER OF RADIO SIGNAL, BASED ON ESTIMATED DISTANCE OR PROPAGATION DELAY



INTERNATIONAL SEARCH REPORT

International application No

PCT/US2022/037622

	FICATION OF SUBJECT MATTER G01S11/08 G01S5/02			
ADD.				
According to	o International Patent Classification (IPC) or to both national classific	cation and IPC		
B. FIELDS	SEARCHED			
Minimum do	ocumentation searched (classification system followed by classificat	tion symbols)		
Documenta	tion searched other than minimum documentation to the extent that	such documents are included in the fields s	earched	
Electronic d	ata base consulted during the international search (name of data ba	ase and, where practicable, search terms us	sed)	
EPO-In	ternal, WPI Data			
C. DOCUM	ENTS CONSIDERED TO BE RELEVANT			
Category*	Citation of document, with indication, where appropriate, of the re	Relevant to claim No.		
A	US 2012/320787 A1 (SUGAR GARY L AL) 20 December 2012 (2012-12-20 figures 1-8		1-24	
A	KR 2018 0044061 A (AGENCY DEFENS [KR]) 2 May 2018 (2018-05-02) paragraph [0002] - paragraph [00		1-24	
A	US 2019/089405 A1 (RYDÉN HENRIK AL) 21 March 2019 (2019-03-21) the whole document 	[SE] ET	1-24	
Furti	ner documents are listed in the continuation of Box C.	X See patent family annex.		
* Special categories of cited documents: "A" document defining the general state of the art which is not considered to be of particular relevance "E" earlier application or patent but published on or after the international filing date "L" document which may throw doubts on priority claim(s) or which is cited to establish the publication date of another citation or other special reason (as specified) "O" document referring to an oral disclosure, use, exhibition or other means "P" document published prior to the international filing date but later than the priority date claimed		 "T" later document published after the international filing date or priority date and not in conflict with the application but cited to understand the principle or theory underlying the invention "X" document of particular relevance;; the claimed invention cannot be considered novel or cannot be considered to involve an inventive step when the document is taken alone "Y" document of particular relevance;; the claimed invention cannot be considered to involve an inventive step when the document is combined with one or more other such documents, such combination being obvious to a person skilled in the art "&" document member of the same patent family 		
Date of the	actual completion of the international search	Date of mailing of the international sea	arch report	
2	7 October 2022	11/11/2022		
Name and r	mailing address of the ISA/ European Patent Office, P.B. 5818 Patentlaan 2 NL - 2280 HV Rijswijk Tel. (+31-70) 340-2040, Fax: (+31-70) 340-3016	Authorized officer Bohnhoff, Peter		

INTERNATIONAL SEARCH REPORT

Information on patent family members

International application No
PCT/US2022/037622

Patent document cited in search report		Publication date		Patent family member(s)		Publication date
US 2012320787	A1	20-12-2012	NONE			
KR 20180044061	A	02-05-2018	NONE			
US 2019089405	A1	21-03-2019	 EP	3437394	A1	06-02-2019
			US	2019089405	A1	21-03-2019
			WO	2017171593	A1	05-10-2017